JACS
JOURNAL OF THE AMERICAN CHEMICAL SOCIETY

Article

pubs.acs.org/JACS

Quantitative Bimolecular Recombination in Organic Photovoltaics through Triplet Exciton Formation

Philip C. Y. Chow, Simon Gélinas, Akshay Rao, and Richard H. Friend*

Cavendish Laboratory, University of Cambridge, J.J. Thomson Avenue, Cambridge, CB3 0HE, United Kingdom

Supporting Information

ABSTRACT: The nanoscale morphology and high charge densities in organic photovoltaics (OPVs) lead to a high rate of bimolecular encounters between spin-uncorrelated electrons and holes. This process can lead to the formation of low-energy triplet excitons on the donor polymer that decay nonradiatively and limit the device performance. We use time-resolved optical spectroscopy to characterize the effect of morphology through the use of solvent additives such as 1,8-octanedithiol (ODT) on triplet dynamics and charge recombination in blends of poly[2,6-(4,4-bis(2-ethylhexyl)-4*H*-cyclopenta[2,1-*b*;3,4-*b*′]-dithiophene)-*alt*-4,7-(2,1,3-benzothiadiazole)] and [6,6]-phenyl-C_{71}-butyric acid methyl ester. This is an attractive OPV system since the extended absorption of the polymer into the near-infrared gives good coverage of the solar spectrum, but nevertheless, the internal quantum efficiency (IQE) has not been reported to be higher than ∼65% under short circuit conditions. We find that, without ODT, the IQE is 48% and 16% of excitations decay via bimolecular triplet formation. With ODT treatment, which improves crystallinity and carrier mobility, the IQE increases to 65%, but bimolecular triplet formation significantly increases and now accounts for all of the recombination (35% of charges).

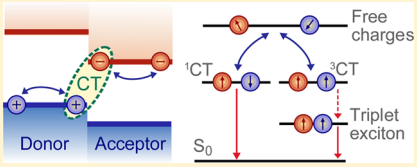

INTRODUCTION

Organic photovoltaics (OPVs) based on solution-processed polymer:fullerene bulk heterojunctions have promising potential to reduce the cost of solar energy. An OPV cell comprises a thin film of a nanostructured blend of two semiconductors, the electron donor (D) and electron acceptor (A), sandwiched between electron- and hole-extracting contacts.[1,2] Due to the low dielectric constant of organic semiconductors, photoexcitation leads to the formation of tightly bound electron−hole pairs, excitons, and an energetic offset at the D−A interface is needed to dissociate these excitons. The dissociation of these excitons forms interfacial charge-transfer (CT) states, which could either (1) relax to bound CT states that undergo geminate recombination or (2) separate to form unbound (free) charge pairs which could be extracted at the electrodes to form a photocurrent. The dynamics of the CT states is therefore critical to the photoconversion efficiency. Recent studies have shown that CT state dynamics are not only determined by the D−A energetic offset but also greatly influenced by the delocalization of its wave function across the interface.[3−5] The probability of forming bound CT states is greatly reduced if the CT states are sufficiently delocalized—a property which is greatly affected by molecular packing and morphology. In polymer:fullerene blends, the CT states are typically sufficiently delocalized such that most photogenerated excitons can be separated into free charge pairs.

While the properties of CT states formed directly from photogenerated excitons are widely considered to be critical for OPV operation, the CT states populated via bimolecular encounters of free charges have been generally neglected. This process should be analogous to the primary operating mechanism of organic light-emitting diodes (OLEDs), where encounters of injected electrons and holes generate CT states with both singlet (^{1}CT) and triplet (^{3}CT) spin characteristics according to spin statistics.[6,7] Recently, we have established that encounters between electrons and holes in polymer:fullerene blends generate CT states of both spins and that these states play an important role in PV operation.[8] This is summarized in Figure 1. The ^{3}CT states can relax to the lower-lying triplet exciton (T_1) state on the donor polymer if it is energetically accessible.[9−11] This is typically the case for blends that employ low-band-gap polymers with absorption extending into the near-infrared, which is ideal for PV operation. The formation of these energetically lower-lying triplets is detrimental to device performance, as they are quickly annihilated by the charge population in the device and thus act as a terminal recombination pathway. However, triplet formation can be suppressed, even when energetically favorable, provided that the CT states are delocalized.[8] This enables CT states to be recycled back to free charges and suppress recombination.

It is thus clear that further improvements in device performance require that this newly established mechanism be fully explored and new design rules formulated. In order to fully understand the role of CT states, triplet excitons, triplet-charge annihilation (TCA), and bimolecular charge recombination on device performance, it is necessary to gain a quantitative understanding of these processes and how they are affected by morphology.

Here we study the dynamics of triplets and their interaction with charges in PCPDTBT:PC_{70}BM, which is a well-studied system with an ideal optical band gap (1.5 eV) and high charge

Received: October 1, 2013
Published: February 12, 2014

   dx.doi.org/10.1021/ja410092n | *J. Am. Chem. Soc.* 2014, 136, 3424−3429

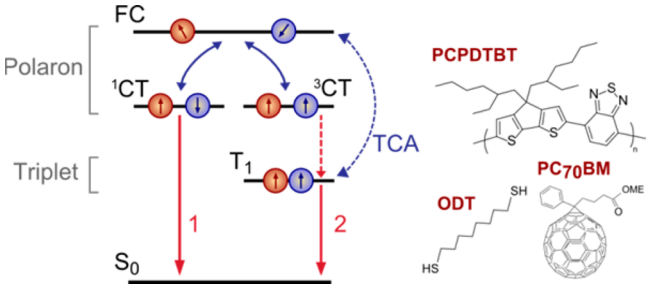

Figure 1. (Left) Schematic of bimolecular recombination processes of free charge carriers (FC) in OPV (not to energy scale). Encounters of spin-uncorrelated charges at D−A interface form charge-transfer states with both singlet (^{1}CT) and triplet (^{3}CT) spin characteristics. These CT states could either reionize into FC or recombine terminally across the interface. Recombination of ^{1}CT to the ground-state S_0 (pathway 1) is spin-allowed and thus could lead to CT state emission. Note that pathway 1 also includes the recombination of bound CT states which never separated into FC (geminate recombination). While direct recombination of ^{3}CT to S_0 (pathway 2) is spin-forbidden, recombination could take place through the formation of energetically lower-lying triplet excitons (T_1) on the donor polymer (provided that $E_{T1} < E_{CT}$). These triplets are rapidly quenched to the ground state through triplet-charge annihilation (TCA). This limits the possibility of triplets to thermalize back into charges, which is thermodynamically feasible in poly[2,6-(4,4-bis(2-ethylhexyl)-4*H*-cyclopenta[2,1-*b*;3,4-*b*′]-dithiophene)-*alt*-4,7-(2,1,3-benzothiadiazole)] (PCPDTBT):[6,6]-phenyl-C_{71}-butyric acid methyl ester ($PC_{70}BM$) blends ($E_{CT} - E_{T1} \sim 200$ meV). Intersystem crossing between CT states (not shown here) has a much slower rate compared to the processes illustrated here. (Right) Molecular structure of the materials used in this study.

mobilities.[12,13] This system allows for the blend morphology to be altered via the use of solvent additives, a topic that has been extensively studied.[11,14−17] The addition of 1,8-octanedithiol (ODT) to the solvent prior to spin-coating coarsens the blend morphology and improves power conversion efficiency by up to a factor of 2.[14] The coarsened morphology allows the formation of pure, crystalline phases of both the polymer and the fullerene that improves charge-carrier separation and mobility.[15,16] As we develop below, the ability to modify the morphology without changing the blend composition allows for a unique window into the role that morphology plays in the interaction of charges and triplet excitons. Di Nuzzo et al. have previously observed the formation of triplet excitons on the polymer upon photoexcitation of the blend, using quasi-steady-state photo-induced absorption (PIA) measurements.[11] They attributed the triplet formation to geminate recombination of CT states that failed to separate into free charges. A weaker triplet signal was measured in the blend processed with ODT, suggesting that triplet formation is suppressed due to the enhanced separation of CT states.

EXPERIMENTAL METHODS

We investigated spin-coated films of PCPDTBT:$PC_{70}BM$ blends on quartz substrates, processed with/without ODT, using transient absorption (TA) spectroscopy. In this technique, an ultrafast pulse generates photoexcitations within the sample. After a certain time delay, we optically probe the excited states within the sample using a broad-band probe pulse (200 fs). Excited states in OPV blends are typically long-lived (up to microsecond time scales) because of efficient charge separation, and it is therefore necessary to have sufficient temporal range in the measurements. We achieved this by employing optically delayed ultrafast pulses for subnanosecond (<2 ns) measurements and electrically delayed nanosecond pulses for measurements from 1 ns up to 1 ms. The excitation wavelength was fixed at 532 nm for consistency.

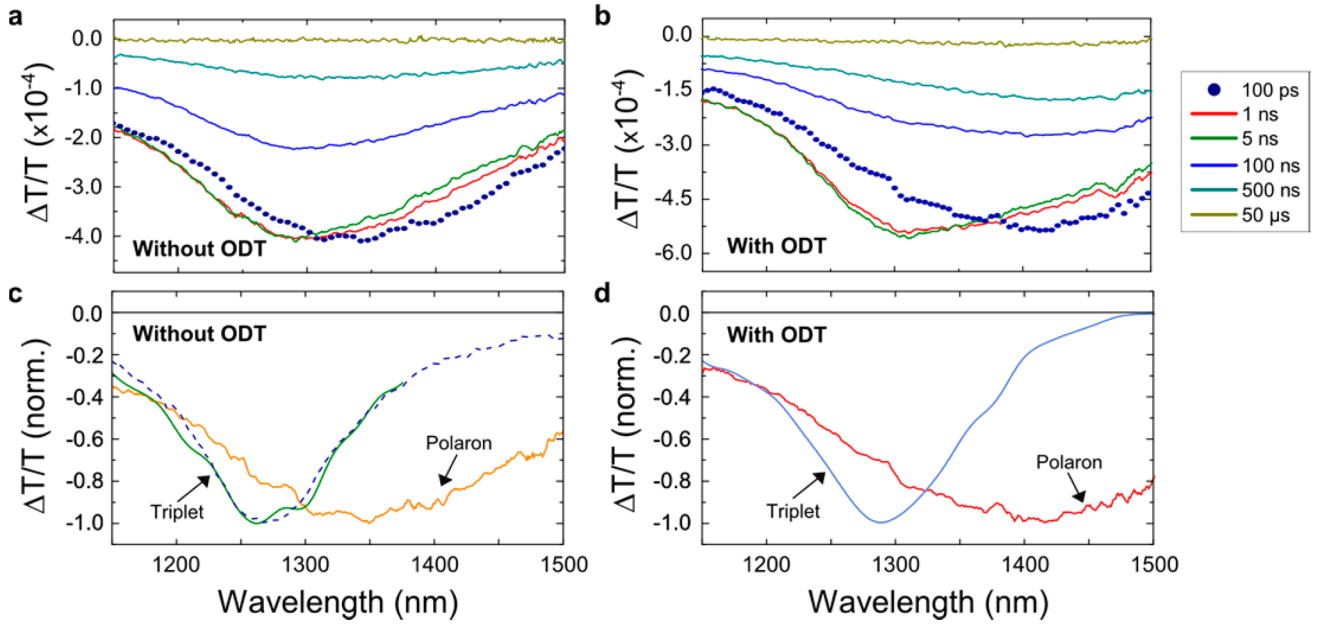

Figure 2. Evolution of transient absorption (TA) spectra in the near-infrared measured for PCPDTBT:$PC_{70}BM$ (1:2) blends processed without (a) and with (b) solvent additive 1,8-octanedithiol (ODT), photoexcited at 532 nm and fluence of 2.4 μJ/cm^2. The solid lines show the spectral evolution from 1 ns, where the samples were photoexcited by electrically delayed pulses with 1 ns pulse width. In order to compare with the spectral feature at earlier time, the spectra measured at 100 ps (using optically delayed pulses with 200 fs pulse width) were plotted for reference (solid dots). (c,d) Normalized polaron and triplet absorption spectra in the respective blends, which were deconvoluted from the spectra shown in (a) and (b) as discussed in the text. The triplet absorption spectra directly measured in a pristine PCPDTBT thin film (at 50 ns time delay) are shown as the blue-dashed line in (c). The emergence of triplet absorption on the nanosecond time scale caused the overall blue shift observed in both blends.

dx.doi.org/10.1021/ja410092n | J. Am. Chem. Soc. 2014, 136, 3424−3429

We employed broad-band probe pulses with spectral range spanning from 550 to 1650 nm, generated using home-built noncollinear optical parametric amplifiers (NOPA).[18] In conjugated polymers, local geometrical relaxation around charges causes rearrangement of energy levels, forming polarons, which brings states into the semiconductor gap with broad optical transitions below the band gap.[19] The near-IR spectral range is therefore necessary for studying the excited-state dynamics in low-band-gap polymer including PCPDTBT. The combination of broad temporal and spectral range enabled us to study the dynamics of excited states in the samples throughout their lifetime.

We ensured that the excitation densities within the blends generated by the excitation pulses were similar to that under solar illumination conditions (10^{16} excitations/cm^3).[20] This is important because higher-order annihilation processes between excitons and charges can dominate at higher excitation densities, making such measurements unreliable indicators of device operation under AM1.5G illumination.[21] A high signal sensitivity level (5×10^{-6}) enabled this in our measurements. Details of sample preparation are described in Supporting Information.

RESULTS AND DISCUSSION

Figure 2 shows the near-infrared (NIR) TA spectra of PCPDTBT:PC$_{70}$BM (1:2) blends spin-casted without (a) and with (b) ODT, photoexcited at 2.4 μJ/cm^2. The spectra consist of a broad photoinduced absorption (PIA) feature. At 100 ps, these spectra peaked at about 1350 and 1420 nm without and with ODT blends, respectively. Both spectra blue-shifted as the time delay was increased to a few nanoseconds, with their peaks almost overlapping at about 1300 nm, before the amplitudes begin to drop. In both cases, we find that the spectral evolution is due to the emergence of an overlapping PIA feature on the nanosecond time scales.

In order to deconvolute the overlapping absorption features and obtain their kinetics, we use numerical methods based on a genetic algorithm.[22] The full detail of this approach can be found in the Supporting Information. The results are summarized in Figure 2c,d for samples without/with ODT, respectively. We extracted two absorption features in both blends. The narrow feature that peaks at shorter wavelength is in good agreement with the absorption of triplet excitons in PCPDTBT shown by Di Nuzzo et al. using steady-state PIA measurements.[11] We further confirmed this by obtaining the triplet absorption spectrum in a pristine PCPDTBT thin film, which appeared as a long-lived signal that decays on the microsecond time scale (see Supporting Information). This is shown as the dashed blue line in Figure 2c, and it is in good agreement with the extracted spectrum. Having confirmed the triplet absorption signatures, we attribute the broad spectral features to the polaron absorption of the respective samples. These polaron absorption features resemble the TA spectra measured at 100 ps in the respective blends. This confirms that charges are the dominant excited species at this time scale formed following the dissociation of photogenerated singlet excitons. The polaron absorption is red-shifted (45 meV) in the blend processed with ODT. Such a shift is also observed in the ground-state absorption (π–π^* transition), which reflects the improved structural order of the polymer phase by the addition of ODT (Figure S1).[14]

Figure 3a shows the evolution of the isolated triplet and polaron absorption signal in PCPDTBT:PC$_{70}$BM blend processed without (top) and with ODT (bottom) from 1 ns onward when photoexcited at three different excitation fluences: 1.2, 2.4, and 4.8 μJ/cm^2. Note that in order to account for the difference in absorbance between the two

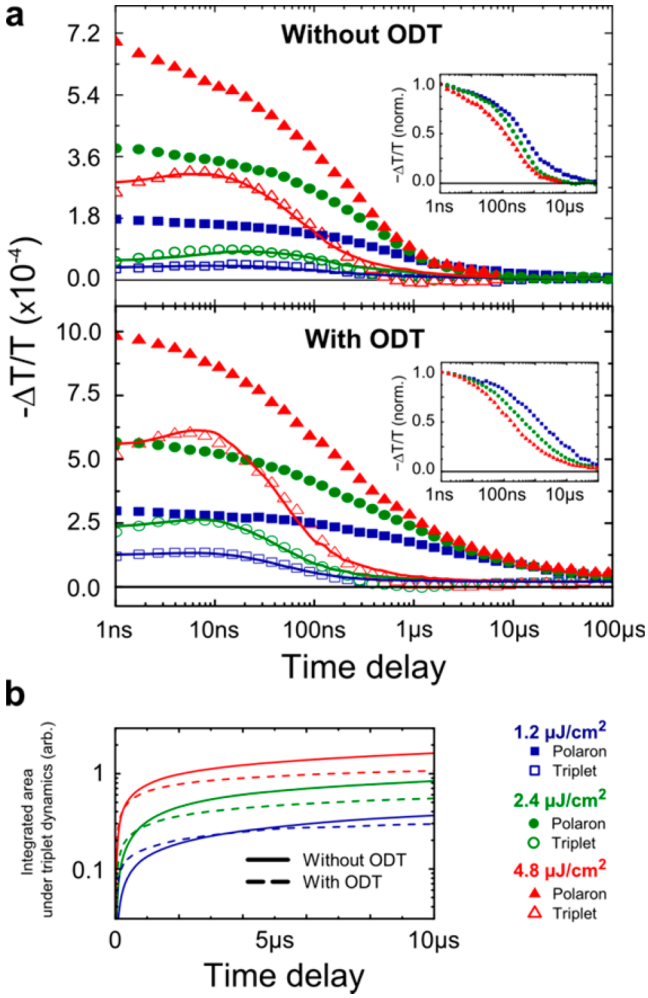

Figure 3. (a) Dynamics of polaron and triplet absorption signals in PCPDTBT:PC$_{70}$BM (1:2) films processed without/with solvent additive ODT, photoexcited at 532 nm and under three excitation fluences. The polaron and triplet absorption signals were deconvoluted as discussed in the text. The data measured in the ODT-processed blend were scaled by a factor of 1.17 to account for the mismatch in absorbance at the excitation wavelength. The normalized polaron kinetics for the respective blend is shown in the insets. The increasing decay rate of polarons at higher fluences indicates that bimolecular recombination is the dominant decay pathway on this time scale. While the polaron signal was increased with the use of ODT throughout the temporal window, consistent with the improved device performance, the peak triplet signal was also increased, indicating that more triplets were formed in this blend. In addition, the triplet dynamics demonstrated faster formation and decay rates in the ODT-processed blend. The solid lines show the fittings of the triplet dynamics using eq 1 (see Table 1 for fitting parameters). (b) Integrated area under triplet dynamics in (a) mimics a quasi-steady-state measurement (in the long-time limit). Under all three fluence conditions, the blend processed with ODT (dashed lines) had a smaller integrated area despite having more triplets formed because of the increased quenching rate.

blends at the excitation wavelength, all the TA data measured for the ODT-processed blend have been scaled by a factor of 1.17. The initial signal of the polaron absorption scaled linearly with fluence, indicating that higher-order annihilation processes involving singlet excitons at earlier times did not affect these measurements. The normalized polaron kinetics is shown in the inset. As discussed by Etzold et al.,[17] the initial fluence-

dx.doi.org/10.1021/ja410092n | J. Am. Chem. Soc. 2014, 136, 3424–3429

independent decay (at low fluences) up to tens of nanoseconds observed without ODT corresponds to the substantial geminate recombination of bound CT states in this blend. With ODT, geminate recombination is suppressed and the charges undergo fluence-dependent decay which corresponds to nongeminate recombination (bimolecular) of free charges.

The triplet kinetics showed an initial increase on the nanosecond time scale before decaying at a much faster rate compared to the charge decay. This emergence of triplet absorption and fall of polaron absorption on the nanosecond time scale caused the overall blue shift of the TA spectra shown in Figure 2a,b. We observed more triplets being formed at higher fluences, and the rate of triplet formation was correlated with the recombination rate of charges in both blends. This indicates that triplets were populated following charge recombination.[8] The triplet lifetime in both blends is much reduced compared to that in neat PCPDTBT film (1 μs)[17] and further decreases at higher fluences. We consider that the decay of triplets is predominantly driven by triplet-charge annihilation,[23,24] in which the triplet is quenched to the ground state, losing its energy to the charge. The rate of TCA scales with fluence because of the increased population densities of charges and triplets. In addition, triplet−triplet annihilation (TTA) could also have resulted in the increased quenching rate at higher fluence. However, we do not consider this as the dominant triplet quenching pathway in these blends because of the lack of delayed fluorescence observed,[25] which could arise from the singlets populated following TTA.[7] We modeled the triplet dynamics using a kinetic model[8] (eq 1)

$$\frac{dN_T}{dt} = -\alpha\frac{dN_C}{dt} - \gamma_{TCA}N_TN_C \quad (1)$$

where N_C and N_T are the charge and triplet population densities, respectively. This model assumes that the triplet dynamics is governed by a single growth and decay term. The growth term is proportional to the recombination of charges with α being the fraction that forms triplets, and the decay is governed by TCA with rate constant γ_{TCA}. The fits to this model are shown as the solid line in Figure 3a and are found to be in good agreement with the data.

Both polaron and triplet dynamics were clearly affected by the use of ODT. The polaron signal was increased with ODT throughout the accessible temporal range and had an extended lifetime, which is consistent with the enhanced device performance. On the other hand, we also observed larger triplet signal in the ODT-processed blend, indicating that more triplets were formed. Besides the higher formation rate, the triplet decay rate was also significantly increased with ODT. These are consistent with the triplet dynamics model described above. The use of ODT causes the formation of purer, crystalline phase of both the polymer and fullerene,[15,16] which subsequently leads to (1) increased charge density due to reduced geminate recombination of bound CT states[17] and (2) enhanced carrier mobilities.[16] The combination of these two factors leads to an increase in bimolecular charge encounters and therefore triplet formation in the ODT-processed blend. In addition to this, having a higher population density with improved mobility of both charges and triplets also increases the rate of TCA and is therefore consistent with the faster quenching rate observed.

The effect of ODT on triplet dynamics observed here is consistent with the quasi-steady-state PIA measurements observed by Di Nuzzo et al.[11] Integrating the time-resolved triplet dynamics presented in Figure 3a mimics the quasi-steady-state measurement. This is shown in Figure 3b, where the area under the triplet dynamics is plotted against time. Under all three excitation fluences, the area increases more rapidly in the ODT-processed blend (dashed lines), demonstrating the faster triplet formation. However, the areas reach a plateau at an earlier time because of the faster triplet quenching rates, while the signals for the untreated blend continue to grow. This explains the lower quasi-steady-state triplet signals observed with ODT, despite more triplets being formed at earlier times.

To quantify the population densities and the fitting parameters in eq 1, the absorption cross sections (σ) of both polaron and triplet states are required, according to $N = (\Delta T/T)/d\sigma$, where d is the thickness of the film. The polaron cross section (σ_C) was determined from the early time (<ns) TA measurements for both blends (Figures S6 and S7). We assume that the polaron population at 100 ps is equal to the number of photons absorbed by the films based on the assumption that all photoexcited singlets dissociated completely across the interface in both blends to form polarons following exciton diffusion. We consider this a reasonable assumption because of the efficient fluorescence quenching demonstrated in these blends.[25] In addition, charge recombination events were found to occur on a longer time scale than 100 ps in these blends.[17] Using this approach, we obtained $\sigma_C = 2.5 \times 10^{-16}$ cm^{-2} ± 5% at the respective polaron absorption peak shown in Figure 2c,d for the two blends.

Determining the triplet cross section (σ_T) is more complicated because it is difficult to accurately estimate the yield of triplets following photoexcitation. Triplet sensitization experiments have been carried out to selectively populate the polymeric triplet state via Dexter-type energy transfer.[26] However, such experiments rely heavily on estimating the ratio of photoexcited states in the sensitizer that ultimately end up in the polymeric triplet state. Here we used two different approaches. First, we photoexcited a dilute solution (100 μg/mL) of PCPDTBT and measured both the ground-state bleach (GSB) and absorption of long-lived triplet excitons on the nanosecond time scale (see Figures S8 and S9). In solution phase, both singlet and triplet excitons are localized on a single polymer chain; we therefore assumed that their GSB values are the same and from which we obtained $\sigma_T = 4.8 \times 10^{-16}$ cm^{-2} ± 10% at the triplet absorption peak (see Figure 2c). Alternatively, we estimated the triplet cross section directly from the dynamics of polarons and triplets in the blended film (Figure S10). For the ODT-processed blend, we assumed that the growth of triplet population is roughly equal to the loss in charge population on the subnanosecond time scale because geminate recombination is strongly suppressed.[17] From this approach, we estimated that the absorption cross section of triplets is roughly a factor of 2 greater than polarons, which is in good agreement with the value obtained from the first approach. Moreover, this value is comparable to the absorption cross sections of triplet excitons previously reported for other push−pull conjugated polymers such as F8BT[27] and F8TBT.[28]

The fitting parameters extracted from the triplet dynamics shown in Figure 3a using the model described in eq 1 are summarized in Table 1, using the polaron and triplet cross sections discussed above. The triplet formation fraction α indicates that three-quarters of charge recombination events led to triplets in the ODT-processed blend, in agreement with spin statistics, and thus confirms that bimolecular recombination of

dx.doi.org/10.1021/ja410092n | J. Am. Chem. Soc. 2014, 136, 3424−3429

Table 1. Quantifying Triplet Dynamics and Charge Recombination in PCPDTBT:$PC_{70}BM$ Films with/without ODT[a]

	without ODT	with ODT
α	0.57	0.76
γ_{TCA} ($cm^3\ s^{-1}$)	8.1×10^{-11}	1.5×10^{-10}
measured IQE	48%	65%
estimated IQE	41 ± 5%	63 ± 5%
recombination via ^{3}CT (pathway 2)	16 ± 5%	37 ± 5%
recombination via ^{1}CT (pathway 1)	43 ± 5%	<5%

[a]The triplet formation fraction (α) and decay rate constant (γ_{TCA}) were extracted from the fitting of triplet dynamics in Figure 3a using eq 1 (with estimated absorption cross sections). The ratio of surviving charges at the extraction time scale (100 ns) measured in thin films provides a reasonable estimate of the short circuit internal quantum efficiency (IQE) of the blends had there been electrodes attached, and this is confirmed by the agreement with the measured IQE of an operating device. We determined the fraction of charges that had recombined bimolecularly to form triplets (pathway 2) by quantifying the total triplet population generated at the extraction time scale if there were no triplet quenching (using the obtained value of α). Having estimated the ratio of photoexcitations that leads to photocurrent and triplets, we consider that the remaining photoexcitations must decay via the ^{1}CT state, which is populated from either direct charge transfer (geminate pair) or bimolecular encounters, either radiatively or nonradiatively (pathway 1).

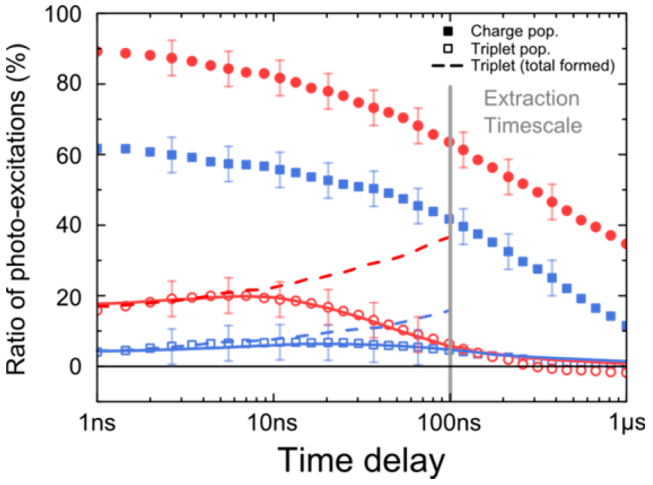

Figure 4. Dynamics of charge and triplet populations as a ratio of photoexcitations initially created in PCPDTBT:$PC_{70}BM$ (1:2) films processed without (blue squares) and with ODT (red circles). Both films were excited at 532 nm at a fluence of 2.4 $\mu J/cm^2$. The population densities of either species were determined using the estimated absorption cross sections as discussed in the text. The extraction time scale (100 ns) was determined based on separate TA measurements on operating devices made with these blends. The charge population at the extraction time scale provides an estimate of the internal quantum efficiency (IQE) of the blends if there were electrodes attached under short circuit conditions. The dashed lines show the total triplet population that would be present in the film if there were no triplet quenching. The total triplet population generated at the extraction time scale corresponds to the ratio of charges which had recombined to form triplets.

free charge to triplets is the dominant loss pathway in this blend. In addition, the 2-fold increase in the triplet decay rate constant γ_{TCA} reflects the enhanced rate of TCA due to the improved carrier mobility through the use of ODT. It is important to note that TCA does not directly affect the charge population because the triplet energy is transferred to the charge during the process.[24] In fact, it could be possible that this process contributes to the separation of bound charges and consequently the photocurrent, but further experiments are required to explore this mechanism. However, the rapid quenching of triplets to the ground state via TCA limits the possibility for triplets to thermalize back into charges, which is thermodynamically feasible given the small energy difference between the triplet state and the CT state (~200 meV) for PCPDTBT:$PC_{70}BM$ blends.[11] Thus, while the use of ODT enhanced charge generation by improving morphology and carrier mobility, it in turn increased the rate of charge recombination through the triplet state.

Finally, we can quantitatively determine the ratio of recombination pathways undertaken by the photogenerated charges in either blends. Using the obtained absorption cross sections of triplets and charges, we deduced the population density of either species as a function of time and normalized it to the number of photoexcitations initially created (see Figure 4). From a separate TA measurement on an operating PCPDTBT:$PC_{70}BM$ device under short circuit conditions, we observed charge extraction from 100 ns onward (Figure S11), with the measured quantum efficiency found to correlate with the charge population at 100 ns. Hence, we consider that the ratio of surviving charges at 100 ns measured in thin films provides a reasonable estimate of the short circuit internal quantum efficiency (IQE) of the blends had there been electrodes attached while neglecting drift-limited processes.[29] This is confirmed by the agreement between the ratio of surviving charges and the measured IQE for both blends (Figure S3), as summarized in Table 1. The measured IQE was determined using the method described by Burkhard et al.[30] (see Supporting Information).

In order to quantify bimolecular triplet formation, we need to consider the total number of triplets formed up to the extraction time scale; that is, we need to know how many charge recombination events led to triplet formation. This cannot be known by looking directly at the actual triplet population, as the triplets are constantly being quenched by TCA. However, TCA does not directly affect triplet formation, which is only dependent on the charge dynamics (eq 1). The dashed lines in Figure 4 plot the sum of the triplet formation (using α in Table 1) up to 100 ns, which corresponds to the total triplet population that would be present in the blends if there was no triplet quenching. The total triplet population generated at the extraction time scale corresponds to the fraction of charges that had recombined bimolecularly to form triplets.

In the untreated blend, recombination through triplets accounts for ~16% of the loss of charges (this is labeled as pathway 2 in Figure 1 and Table 1). Having estimated the ratio of photoexcitations that leads to photocurrent (~41%) and triplets (~16%), we consider that the remaining photoexcitations (~43%) must decay via the ^{1}CT state, which is populated from either direct charge transfer (geminate pair) or bimolecular encounters, either radiatively or nonradiatively (this is labeled as pathway 1 in Figure 1 and Table 1). On the other hand, while the IQE increases to 65% with ODT treatment, recombination through triplets also increases to ~35% of the charges, accounting for all of the recombination in this blend. This demonstrates that while improving phase crystallinity and carrier mobility leads to better charge

dx.doi.org/10.1021/ja410092n | J. Am. Chem. Soc. 2014, 136, 3424−3429

generation, these can in turn increase recombination to form triplets, which act as a terminal loss pathway because triplets are rapidly quenched by TCA.

Finally, we note that although the improved phase crystallinity obtained through the use of ODT improves device performance considerably, it does not completely suppress the bimolecular recombination via triplets. This is in contrast to highly efficient systems such as PIDT-PhanQ:PCBM,[8] where the formation of PCBM clusters[31,32] shuts down recombination via triplets. These results suggest that the presence of PCBM clusters is a necessary, but not sufficient, condition to avoid recombination through triplet formation. It is likely that the nature of PCBM clusters (size, crystallinity, etc.) is highly dependent on the polymer with which it is blended. Further structural studies are called for to fully understand what factors lead to optimal morphologies to avoid bimolecular triplet formation.

CONCLUSION

We have elucidated and quantified the recombination pathways that limit the power conversion efficiency of PCPDTBT:$PC_{70}BM$ blends even after the optimization of blend morphology through the use of solvent additives. This finding indicates that OPV blends that possess high phase crystallinity and carrier mobilities do not necessarily make a good solar cell since recombination could take place through the lower-lying triplet exciton states. Instead, as we have shown elsewhere,[8] the use of blends with sufficiently delocalized interfacial states allows rapid thermalization of CT states with both spin-singlet and spin-triplet characteristics and thus enables both recombination pathways to be significantly suppressed.

ASSOCIATED CONTENT

Supporting Information

Additional information on sample preparation, UV−vis absorption, device characterization, genetic algorithm, and other TA characterization on pristine polymer, blends, and devices. This material is available free of charge via the Internet at http://pubs.acs.org.

AUTHOR INFORMATION

Corresponding Author

rhf10@cam.ac.uk

Notes

The authors declare no competing financial interest.

ACKNOWLEDGMENTS

This work was supported by the Engineering and Physical Sciences Research Council (EPSRC).

REFERENCES

(1) Yu, G.; Gao, J.; Hummelen, J. C.; Wudl, F.; Heeger, A. J. *Science* **1995**, *270*, 1789.
(2) Halls, J. J. M.; Walsh, C. A.; Greenham, N. C.; Marseglia, E. A.; Friend, R. H.; Moratti, S. C.; Holmes, A. B. *Nature* **1995**, *376*, 498.
(3) Bakulin, A. A.; Rao, A.; Pavelyev, V. G.; van Loosdrecht, P. H. M.; Pshenichnikov, M. S.; Niedzialek, D.; Cornil, J.; Beljonne, D.; Friend, R. H. *Science* **2012**, *335*, 1340.
(4) Bakulin, A. A.; Dimitrov, S. D.; Rao, A.; Chow, P. C.; Nielsen, C. B.; Schroeder, B. C.; McCulloch, I.; Bakker, H. J.; Durrant, J. R.; Friend, R. H. *J. Phys. Chem. Lett.* **2012**, *4*, 209.
(5) Jamieson, F. C.; Domingo, E. B.; McCarthy-Ward, T.; Heeney, M.; Stingelin, N.; Durrant, J. R. *Chem. Sci.* **2012**, *3*, 1.
(6) Baldo, M. A.; O'Brien, D. F.; Thompson, M. E.; Forrest, S. R. *Phys. Rev. B* **1999**, *60*, 14422.
(7) Wallikewitz, B. H.; Kabra, D.; Gélinas, S.; Friend, R. H. *Phys. Rev. B* **2012**, *85*, 045209.
(8) Rao, A.; Chow, P. C. Y.; Gélinas, S.; Schlenker, C. W.; Li, C.-Z.; Yip, H.-L.; Jen, A. K.-Y.; Ginger, D. S.; Friend, R. H. *Nature* **2013**, *500*, 435.
(9) Dyer-Smith, C.; Reynolds, L. X.; Bruno, A.; Bradley, D. D. C.; Haque, S. A.; Nelson, J. *Adv. Funct. Mater.* **2010**, *20*, 2701.
(10) Westenhoff, S.; Howard, I. A.; Hodgkiss, J. M.; Kirov, K. R.; Bronstein, H. A.; Williams, C. K.; Greenham, N. C.; Friend, R. H. *J. Am. Chem. Soc.* **2008**, *130*, 13653.
(11) Di Nuzzo, D.; Aguirre, A.; Shahid, M.; Gevaerts, V. S.; Meskers, S. C. J.; Janssen, R. A. J. *Adv. Mater.* **2010**, *22*, 4321.
(12) Mühlbacher, D.; Scharber, M.; Morana, M.; Zhu, Z.; Waller, D.; Gaudiana, R.; Brabec, C. *Adv. Mater.* **2006**, *18*, 2884.
(13) Lenes, M.; Morana, M.; Brabec, C. J.; Blom, P. W. M. *Adv. Funct. Mater.* **2009**, *19*, 1106.
(14) Peet, J.; Kim, J. Y.; Coates, N. E.; Ma, W. L.; Moses, D.; Heeger, A. J.; Bazan, G. C. *Nat. Mater.* **2007**, *6*, 497.
(15) Lee, J. K.; Ma, W. L.; Brabec, C. J.; Yuen, J.; Moon, J. S.; Kim, J. Y.; Lee, K.; Bazan, G. C.; Heeger, A. J. *J. Am. Chem. Soc.* **2008**, *130*, 3619.
(16) Agostinelli, T.; Ferenczi, T. A.; Pires, E.; Foster, S.; Maurano, A.; Müller, C.; Ballantyne, A.; Hampton, M.; Lilliu, S.; Campoy Quiles, M. *J. Polym. Sci., Part B: Polym. Phys.* **2011**, *49*, 717.
(17) Etzold, F.; Howard, I. A.; Forler, N.; Cho, D. M.; Meister, M.; Mangold, H.; Shu, J.; Hansen, M. R.; Müllen, K.; Laquai, F. *J. Am. Chem. Soc.* **2012**, *134*, 10569.
(18) Cirmi, G.; Brida, D.; Manzoni, C.; Marangoni, M.; De Silvestri, S.; Cerullo, G. *Opt. Lett.* **2007**, *32*, 2396.
(19) Brazovskii, S. A.; Kirova, N. N. *JETP Lett.* **1981**, *33*, 4.
(20) Credgington, D.; Hamilton, R.; Atienzar, P.; Nelson, J.; Durrant, J. R. *Adv. Funct. Mater.* **2011**, *21*, 2744.
(21) Hodgkiss, J. M.; Albert-Seifried, S.; Rao, A.; Barker, A. J.; Campbell, A. R.; Marsh, R. A.; Friend, R. H. *Adv. Funct. Mater.* **2012**, *22*, 1567.
(22) Gélinas, S.; Paré-Labrosse, O.; Brosseau, C.-N.; Albert-Seifried, S.; McNeill, C. R.; Kirov, K. R.; Howard, I. A.; Leonelli, R.; Friend, R. H.; Silva, C. *J. Phys. Chem. C* **2011**, *115*, 7114.
(23) Hoffmann, S. T.; Athanasopoulos, S.; Beljonne, D.; Bässler, H.; Köhler, A. *J. Phys. Chem. C* **2012**, *116*, 16371.
(24) Howard, I. A.; Hodgkiss, J. M.; Zhang, X.; Kirov, K. R.; Bronstein, H. A.; Williams, C. K.; Friend, R. H.; Westenhoff, S.; Greenham, N. C. *J. Am. Chem. Soc.* **2010**, *132*, 328.
(25) Jarzab, D.; Cordella, F.; Gao, J.; Scharber, M.; Egelhaaf, H.-J.; Loi, M. A. *Adv. Energy Mater.* **2011**, *1*, 604.
(26) Köhler, A.; Bässler, H. *Mater. Sci. Eng., R* **2009**, *66*, 71.
(27) Yang, X.; Lee, C.-L.; Westenhoff, S.; Zhang, X.; Greenham, N. C. *Adv. Mater.* **2009**, *21*, 916.
(28) Ford, T.; Avilov, I.; Beljonne, D.; Greenham, N. *Phys. Rev. B* **2005**, *71*, 125212.
(29) Koster, L.; Smits, E.; Mihailetchi, V.; Blom, P. *Phys. Rev. B* **2005**, 72.
(30) Burkhard, G. F.; Hoke, E. T.; McGehee, M. D. *Adv. Mater.* **2010**, *22*, 3293.
(31) Collins, B. A.; Li, Z.; Tumbleston, J. R.; Gann, E.; McNeill, C. R.; Ade, H. *Adv. Energy Mater.* **2013**, *3*, 65.
(32) Liu, F.; Gu, Y.; Jung, J. W.; Jo, W. H.; Russell, T. P. *J. Polym. Sci., Part B: Polym. Phys.* **2012**, *50*, 1018.